ISSN (Print) : 0974-6846
Indian Journal of Science and Technology, Vol 8(24), DOI: 10.17485/ijst/2015/v8i24/80153, September 2015 ISSN (Online) : 0974-5645

Sparse Banded Matrix Filter for Image Denoising

V. Sowmya*, **Neethu Mohan and K. P. Soman**

Centre for Excellence in Computational Engineering and Networking, Amrita Vishwa Vidyapeetham, Amrita Nagar, Coimbatore – 641112, Tamil Nadu, India; v_sowmya@cb.amrita.edu, neethumohan.ndkm@gmail.com, kp_soman@amrita.edu

Abstract

Noise is one of the prime factors which degrade the quality of an image. Hence, image denoising is an essential image enhancement technique in the image processing domain. In this paper, we use low-pass sparse banded filter matrices for image denoising. Sparsity is the key concept in this filter design. We applied the designed low-pass filter both row-wise and column-wise to denoise the image. The proposed method is experimented on standard test images corrupted with different types of noises namely Gaussian, White Gaussian, Salt & Pepper and Speckle with noise level equals to 0.01, 0.05 and 0.1. The effectiveness of the proposed method of denoising is evaluated by the computation of standard quality metric known as Peak Signal-to-Noise Ratio (PSNR). The experimental result analysis shows that the proposed image denoising technique based on sparse banded filter matrices results in significant improvement in PSNR around 2dB to 8dB for different type of noises with noise level equal to 0.1 and is also aided by the visual analysis.

Keywords: Image Denoising, Low-pass Filter, Noise, Sparse Banded Filter

1. Introduction

The digital images are usually corrupted with noises due to various sources such as, image acquisition, background illuminations, sensors, processors and transmission channels. All these kind of noises will degrade the quality of the images. Image denoising is the process of removing noisy content from the images in order to improve the quality of the images for further processing. Image denoising is an essential requirement in medical diagnosis[1]. It is widely exploited for processing satellite images, since those images are usually corrupted with high degree of noises[2]. The noise level in each bands are different in hyperspectral images and hence the denoising is a complicated task in hyperspectral imagery[3]. The document images have complex background non uniform illumination and noises. Hence image denoising techniques are applied in Optical Character Recognition (OCR)[4]. Video analysis, object recognition, image restoration, image segmentation and pattern analysis are some of the domains which require efficient noise removal.

Image denoising is a wide area of research and several algorithmic approaches have been proposed for denoising the images. A modified non-local means method for ultrasound image denoising is proposed[1]. An image denoising algorithm based on non-local thresholding and wavelet domain shrinkage is used for Synthetic Aperture Radar (SAR) image denoising[2]. A noise adjusted iterative low rank matrix approximation for hyperspectral image denoising is proposed[3]. An iterative regularized framework is adopted in this approach for noise removal. A discrete curvelet transform based image denoising is proposed for OCR applications[4]. The sparse representation and edge preservation capability of curvelet transform is used for background noise removal from OCR images. The concept of wavelet transforms along with wavelet shrinkage and thresholding techniques are widely utilized for image denoising purpose[5,6]. The sparsity based dictionary approach is greatly employed in image denoising framework[7,8]. Three dimensional over complete wavelet dictionary based hyper spectral image denoising is proposed in[9]. Multi scale sparse representation method with non-separable wavelet is used for image denoising[10].

*Author for correspondence

An over complete dictionary based image denoising algorithm combined with K-SVD and OMP is used for image denoising[11]. An image denoising method based on Markov Random Field (MRF) and Maximum a Posteriori (MAP) is proposed[12]. MRF is a two dimensional random process defined on a discrete lattice. In[13], an impulse-mowing anisotropic diffusion filter is used for noise removal. This filter approach has been efficiently applied for removing combined Gaussian noise and random valued impulses. A Filtering-Direction-Controlled Digital Total-Variation Filter (FDC-DTVF) approach for real time denoising is proposed[14]. Qiang Guo et al[15]. proposed a Singular Value Decomposition (SVD) based method for efficient image denoising. Non-local self similarity and low-rank approximation are used here for denoising task. In[16], Jussi Maatta et al. developed an iterated median filter approach with automatic window selection for image noise removal. In[17], bi-dimensional empirical mode decomposition is exploited for the denoising purpose of Ground Penetrating Radar (GPR) images. An image denoising techniques for under water images based on adaptive wavelet transform and adaptive thresholding is proposed[18].

In this paper, we applied low-pass sparse banded filter matrices designed by Selesnick et al.[19] for image denoising. We applied the designed low-pass filter both row-wise and column-wise to denoise the image. The proposed method is experimented on standard test images corrupted with different types of noises with varying noise level. The effectiveness of the proposed method of denoising is evaluated by visual effect and by the computation of standard quality metric known as Peak Signal-to-Noise Ratio (PSNR).

2. Proposed Method for Image Denoising

The proposed method uses the sparse banded filter matrices designed by Selesnick et al.[19] to remove the noise from the images. In this section, the sparse banded low pass filter design is discussed followed by the proposed image denoising technique.

2.1 Banded Filter Matrices

The design and implementation of zero-phase non-causal recursive high-pass and low-pass filters in terms of banded matrices are well explained in [19].

Let us consider the difference equation of the first-order Butterworth high-pass filter as,

$$a_0 y(n) + a_1 y(n-1) = x(n) - x(n-1) \tag{1}$$

where $x(n)$, $y(n)$ are the sequence of input signal and the filter output respectively.

This can be written in matrix form as,

$$Ay = Bx \tag{2}$$

$$\mathrm{A} = \begin{bmatrix} a_0 & & & & & \\ a_1 & a_0 & & & & \\ & \cdot & \cdot & & & \\ & & \cdot & \cdot & & \\ & & & a_1 & a_0 & \\ & & & & a_1 & a_0 \end{bmatrix} \tag{3}$$

$$\mathrm{B} = \begin{bmatrix} -1 & 1 & & & & \\ & -1 & 1 & & & \\ & & \cdot & \cdot & & \\ & & & \cdot & \cdot & \\ & & & & -1 & 1 \end{bmatrix} \tag{4}$$

where A and B are the banded matrices of size $(N-1) \times (N-1)$ and $(N-1) \times (N)$ respectively, is given in (3) and (4) respectively. The length of the input signal is represented by N.

The filter output y of size $((N-1) \times 1)$ can be obtained for the input signal x by,

$$y = A^{-1} Bx \tag{5}$$

The transfer function of the zero-phase non-causal higher-order (d) high-pass Buttterworth filter is,

$$H(z) = \frac{B(z)}{A(z)} = \frac{(-z+2-z^{-1})^d}{(-z+2-z^{-1})^d + \alpha(z+2+z^{-1})^d} \tag{6}$$

The above equation can also be written as,

$$H(z) = 1 - \frac{\alpha(-z+2-z^{-1})^d}{(-z+2-z^{-1})^d + \alpha(z+2+z^{-1})^d} \tag{7}$$

The frequency response of this filter is unity gain at $\omega = \pi$, since the second term of the numerator becomes zero when z =–1, and its first 2d-1 derivatives are zero there. Therefore, the frequency response is maximally flat at $\omega = 0$, hence this is a zero-phase digital filter.

The filter is defined by the positive integer d and by α. The parameter α can be set so that the frequency response has a specified cut-off frequency ω_c.

Solving for α gives,

$$\alpha = \left(\frac{(1-\cos\omega_c)}{(1+\cos\omega_c)} \right)^d \tag{8}$$

Based on the high-pass filter given in (7), the low pass filter $L(z) = 1 - H(z)$ has the transfer function,

$$L(z) = 1 - \frac{\alpha(-z+2-z^{-1})^d}{(-z+2-z^{-1})^d + \alpha(z+2+z^{-1})^d} \tag{9}$$

with a 2d-order zero at z = −1. The low-pass filter equation is given by,

$$y = \hat{x} - A^{-1}Bx \tag{10}$$

The zero-phase low-pass Butterworth filter given in (9) can be implemented using (10). B is a banded sparse matrix of size $(N - 2d) \times (N)$; A is a square symmetric banded sparse matrix of size $(N - 2d) \times (N - 2d)$. Both the sparse banded matrices have d diagonals above and below the main diagonal. The dimension of $\hat{x}$ is $(N - 2d) \times 1$. $\hat{x}$ is obtained by removing first d samples and last d samples from x.

2.2 Image Denoising using Sparse Banded Filter Matrices

In the proposed method, the sparse banded low-pass filter is applied row-wise and column-wise to remove the noise in the image. The block diagram of the proposed methodology of image denoising is shown in Figure 1.

The proposed method consists of the following steps:

- Let us consider an input image $x \in R^{M\times N}$, whose row and column is represented as $x_r \in R^N$ and $x_c \in R^M$ respectively.
- The input image is subjected to border repetition, which is represented by $x \in R^{(M+2d)\times(N+2d)}$, where d refers to the order of the filter. Therefore, the size of sparse banded matrices A and B is $(N \times N)$ and $(N \times (N+2d))$ respectively.

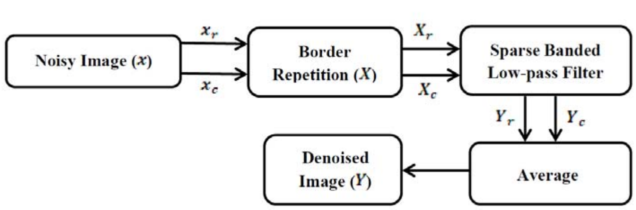

Figure 1. Block diagram of the proposed method of image denoising.

- Each row of the image represented as $X_r \in R^{(N+2d)}$, is passed as an input to the (10) to obtain the filter output, $y_r \in R^N$.

$$y_r = x_r - A^{-1}BX_r \tag{11}$$

- The above step is repeated for all the rows in the input image and is represented as, $Y_r \in R^{M\times N}$.
- The same procedure (steps (3)-(4)) is repeated for each column of the image, $X_c \in R^{(M+2d)}$.
- The filter output sequence for each column is mathematically expressed as $y_r \in R^N$, where

$$y_c = x_c - A^{-1}BX_c \tag{12}$$

- All the columns operated in the image are represented as $Y_c \in R^{M\times N}$.
- The denoised output image is obtained by,

$$Y = \frac{(Y_r + Y_c)}{2} \tag{13}$$

3. Experimental Results and Analysis

In our proposed method, the low-pass sparse banded matrix filter is used for image denoising. The filter is designed with the following input parameters: degree = 2, cut-off frequency = 0.9 and length of sequence = 262. The experiment is performed on various standard images namely, cameraman, Lena, peppers, Barbara, boat and house. The different noise type considered are Gaussian, White Gaussian, Speckle and Salt & Pepper with different noise level equal to 0.01 0.05 and 0.1. The specified noise levels indicates the mean values in the case of Gaussian noise with variance equal to 0.01. In case of White Gaussian and Speckle noise, the noise level refers to local variance with zero mean. The noise density of the Salt & Pepper noise is defined by the noise level.

All the input noisy images are resized to 256 × 256 . To match the input length sequence to the filter, the input image is converted to 262 × 262 by border repetition. The denoised output obtained by our proposed technique for different noises on various standard images with noise level 0.1 is shown in Figure 2– Figure 7. The visual effect of the proposed method for image denoising is aided by the quality metric measurement. The Peak-Signal-to-Noise Ratio (PSNR) computed for different noises with noise level 0.01,0.05 and 0.1 for various standard images are tabulated in Table 1– Table 3.

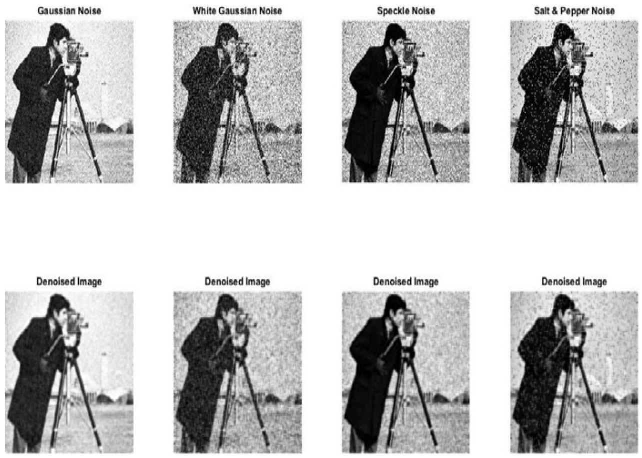

Figure 2. Denoised output of cameraman image for different noises with noise level = 0.1.

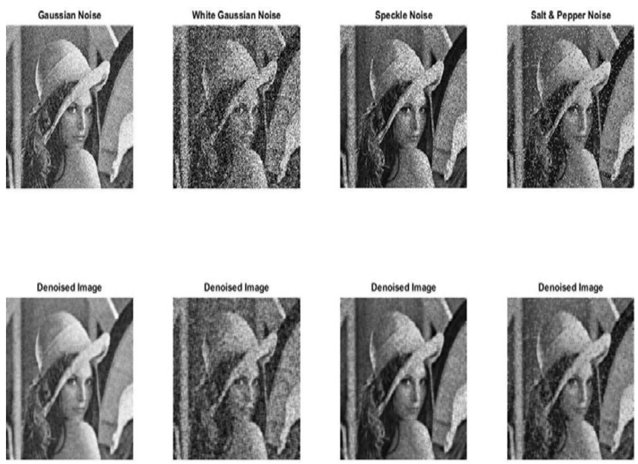

Figure 3. Denoised output of Lena image for different noises with noise level = 0.1.

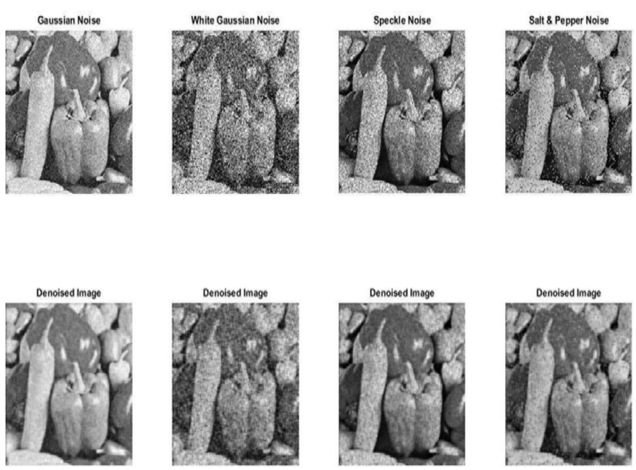

Figure 4. Denoised output of peppers image for different noises with noise level = 0.1.

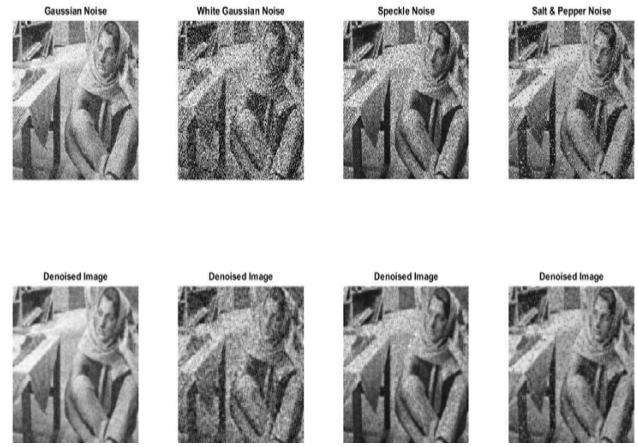

Figure 5. Denoised output of Barbara image for different noises with noise level = 0.1.

Figure 6. Denoised output of boat image for different noises with noise level = 0.1.

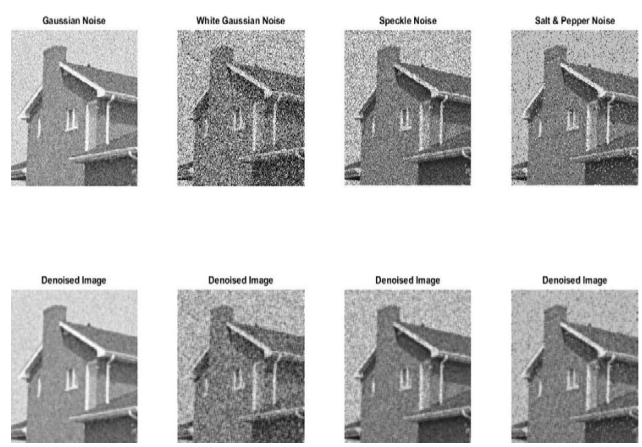

Figure 7. Denoised output of house image for different noises with noise level = 0.1.

Table 1. Peak Signal-to-Noise Ratio (PSNR) for different noises with noise level = 0.01 on standard images

Noise Type	Cameraman		Lena		Peppers		Barbara		Boat		House	
	Noise	Denoise	Noise	Denoise	Noise	Denoise	Noise	Denoise	Noise	Denoise	Noise	Denoise
Gaussian	20.74	**23.96**	20.08	**25.81**	20.08	**26.62**	20.05	**25.78**	20.06	**25.67**	19.96	**27.52**
White Gaussian	20.81	**24.11**	20.24	**26.09**	20.18	**26.79**	20.13	**25.99**	20.08	**25.81**	20.06	**27.77**
Speckle	24.05	**24.98**	27.17	**28.10**	25.75	**28.97**	25.96	**27.70**	25.39	**27.43**	24.91	**30.37**
Salt & Pepper	24.46	**25.19**	25.23	**27.73**	25.55	**28.87**	25.44	**27.59**	25.54	**27.41**	25.36	**30.47**

Table 2. Peak Signal-to-Noise Ratio (PSNR) for different noises with noise level = 0.05 on standard images

Noise Type	Cameraman		Lena		Peppers		Barbara		Boat		House	
	Noise	Denoise	Noise	Denoise	Noise	Denoise	Noise	Denoise	Noise	Denoise	Noise	Denoise
Gaussian	19.72	**22.06**	19.16	**23.02**	19.14	**23.43**	19.17	**23.03**	19.12	**22.98**	19.13	**23.85**
White Gaussian	14.63	**22.61**	13.85	**21.75**	13.74	**22.05**	13.72	**21.78**	13.56	**21.67**	13.64	**22.50**
Speckle	17.75	**22.85**	20.27	**26.15**	18.89	**26.18**	19.15	**25.51**	18.44	**25.00**	18.02	**26.23**
Salt & Pepper	17.31	**22.78**	18.14	**24.86**	18.30	**25.50**	18.32	**24.83**	18.46	**24.82**	18.44	**26.37**

Table 3. Peak Signal-To-Noise Ratio (PSNR) for different noises with noise level = 0.1 on standard images

Noise Type	Cameraman		Lena		Peppers		Barbara		Boat		House	
	Noise	Denoise	Noise	Denoise	Noise	Denoise	Noise	Denoise	Noise	Denoise	Noise	Denoise
Gaussian	17.85	**19.09**	17.02	**19.02**	17.07	**19.24**	17.14	**19.12**	17.06	**19.05**	17.14	**19.43**
White Gaussian	12.19	**18.36**	11.55	**19.50**	11.41	**19.75**	11.41	**19.59**	11.23	**19.46**	11.35	**20.17**
Speckle	15.22	**25.17**	17.44	**24.57**	16.10	**24.09**	16.34	**23.76**	15.53	**23.20**	15.37	**23.84**
Salt & Pepper	14.45	**20.90**	15.20	**22.72**	15.33	**23.16**	15.26	**22.73**	15.37	**22.78**	15.51	**23.89**

From the experimental result analysis, it is evident that the proposed denoising technique removes the various types of noise with noise level less than or equal to 0.1. From Table 1, it is evident that the proposed denoising methodology results in the significant improvement in PSNR for different noises on various standard images with noise level equal to 0.01. The PSNR improvement is around 5db for Gaussian and White Gaussian and 3dB for Speckle and Salt and Pepper noise.

The proposed method is experimented for different noises on various standard images with noise level equal to 0.05. The PSNR value is increased around 2 dB for Gaussian noise, 6dB for White Gaussian noise, 7dB for Speckle and 8dB for Salt and Pepper noise with noise level equal to 0.05 for various standard images, which is tabulated in Table 2.

Similarly, Table 3 shows that for noise level equal to 0.1, the PSNR value is improved around 2dB, 8dB and 7dB for Gaussian, White Gaussian, Speckle and Salt & Pepper noise respectively. Figure 2 – Figure 7 shows the visual emphasis of the quality metric computed for the proposed method experimented for different noises on various standard images with noise level equal to 0.1 tabulated in Table 3.

4. Conclusion

Image denoising based on sparse banded filter matrices is proposed in this paper. The designed filter is applied row-wise and column-wise to denoise the image. The proposed technique is experimented on standard test images subjected to different noises with varying noise level. The effectiveness of denoising by our proposed technique is proved by the significant improvement in standard quality metric known as PSNR aided by the visual analysis.

5. References

1. De Fontes FPX, Barroso GA, Coupe P, Hellier P.Real time ultrasound image denoising. Journal of Real-Time Image Processing. 2011; 6(1):15–22.
2. Sara P, Poderico M, Angelino CV, Verdoliva L. A nonlocal SAR image denoising algorithm based on LLMMSE wavelet shrinkage. IEEE Transactions on Geoscience and Remote Sensing. 2012; 50(2):606–16.
3. He W, Zhang H, Zhang L, Shen H. Hyperspectral image denoising via noise-adjusted iterative low-rank matrix approximation. IEEE Journal on Selected Topics in Applied Earth Observations and Remote Sensing. 2015. p. 1–12.
4. Patvardhan C, Verma AK, Vasantha Lakshmi C. Document image denoising and binarization using Curvelet transform for OCR applications. IEEE Nirma University International Conference on Engineering (NUiCONE); 2012. p. 1–6.
5. Zhao S, Yuanpeng L. A novel image denosing scheme via combining dual-tree complex wavelet transform and bandelets. 3rd International Symposium on Intelligent Information Technology Application (IITA); 2009. p. 509–12.
6. Yin S, Cao L, Ling Y, Jin G. Image denoising with anisotropic bivariate shrinkage. Signal Processing. 2011; 91(8):2078–90.
7. Yang R, Ren M. Learning overcomplete dictionaries with application to image Denoising. Symposium on Photonics and Optoelectronic (SOPO); 2010. p. 1–4.
8. Huang D-E, Kang L-W, Wang Y-CF, Lin C-W. Self-learning based image decomposition with applications to single image denoising. IEEE Transactions on Multimedia. 2014; 16(1):83–93.
9. Rasti B, Sveinsson JR, Ulfarsson MO, Benediktsson JA. Hyperspectral image denoising using 3D wavelets. IEEE International Geoscience and Remote Sensing Symposium (IGARSS); 2012. p. 1349–52.
10. Zeng W, Zhou L, Xu R, Li B. Multi-scale sparse denoising model based on non-separable wavelet. IEEE International Conference on Security, Pattern Analysis and Cybernetics (SPAC); 2014. p. 332–6.
11. Chen Y, Zhan Y. A fast image denoising algorithm via over-complete dictionary. IEEE International Conference on Progress in Informatics and Computing (PIC); 2014. p. 321–5.
12. Suresh KV. Image denoising: A DAMRF model. IEEE 5th International Conference on Signal and Image Processing (ICSIP); 2014. p. 30–5.
13. Kim H, Kim S. Impulse-mowing anisotropic diffusion filter for image denoising. IEEE International Conference on Image Processing (ICIP); 2014. p. 2923–7.
14. Kenta S, Toda M, Tsukada M. Efficient implementation of filtering-direction-controlled digital TV filter for image denoising. IEEE International Conference on Consumer Electronics (ICCE); 2014. p. 633–4.
15. Guo Q, Zhang C, Zhang Y, Liu H. An Efficient SVD-Based Method for Image Denoising. IEEE Transactions on Circuits and Systems for Video Technology. 2015; p. 1.
16. Maatta J, Siltanen S, Roos T. A fixed-point image denoising algorithm with automatic window selection. Proceedings of the 5th European Workshop on Visual Information Processing (EUVIP); 2014.
17. Gan L, Zhou L, You X. A new GPR image de-nosing method based on BEMD. IEEE International Conference on Security, Pattern Analysis and Cybernetics (SPAC); 2014. p. 328–31.
18. Gan L, Zhou L, You X. The research of underwater image de-noising method based on adaptive wavelet transform. IEEE 26th Chinese Control and Decision Conference (CCDC); 2014. p. 2521–5.
19. Selesnick IW, Graber HL, Pfeil DS, Barbour RL. Simultaneous low-pass filtering and total variation denoising. IEEE Transactions on Signal Processing. 2014. p. 1109–24.